

solidus determinations. The magnitude of Fe-loss from the sample in these runs, was quantitatively determined and found to be of minor importance. In subsolidus experiments the results of runs in graphite and in platinum capsules were mutually consistent.

Samples were examined optically and by X-ray powder diffraction. Orthopyroxene forms quite large tabular porphyroblasts; garnet is commonly subhedral but contains many inclusions at lower temperatures and olivine and clinopyroxene form small anhedral grains. Spinel occurs as small, equant, green, isotropic grains and differs from ilmenite (ilmenite + geikielite solid solution) in that the latter is commonly elongate, brown, translucent and with high birefringence. The orthopyroxene crystals are readily analyzed by electron microprobe techniques and some data have been

obtained on olivine, clinopyroxene and garnet compositions. Microprobe analyses for Fe, Ca, Al and Cr were carried out by the methods previously reported [9] using glasses of orthopyroxene composition, analyzed olivines and analyzed garnets as standards.

3. EXPERIMENTAL RESULTS

The results of the determination of the stability field for garnet pyrolite are presented in fig. 1. The data points denote the phase assemblages present in pyrolite III composition. Plagioclase pyrolite is stable under dry conditions on the low pressure side of AB. Between AB and ELF, both garnet and plagioclase are absent and the mineral assemblage is dominated by aluminous pyroxenes. Within this field, spinel is present as a minor phase at temperatures below the line marked K but only olivine, aluminous pyroxenes and accessory ilmenite are present at higher temperatures. Garnet first appears in trace amounts along the line ELF and, at a given temperature, steadily increases in abundance as pressure increases.

The data points for pyrolites I and II are not shown in fig. 1 but in these compositions the first appearance of garnet is along EJ and spinel remains a stable phase up to solidus temperatures on the low pressure side of EJ. Garnet and spinel co-exist together over a very small pressure interval on the high pressure side of EJ. The triangular P, T field FLJ is one in which the olivine + aluminous pyroxenes assemblage is stable in pyrolite III but olivine + aluminous pyroxenes + garnet is stable in pyrolites I and II.

The microprobe analyses so far carried out clearly demonstrate the important role that $(Ca, Mg)Al_2SiO_6$ solid solution in the pyroxenes plays in determining the phase assemblages. The Al_2O_3 contents of orthopyroxene in some of the runs are listed in table 2. The orthopyroxene at $1500^\circ C$ also contains 0.7 - 0.9% Cr_2O_3 in solid solution. Co-existing clinopyroxene contains higher Al_2O_3 and Cr_2O_3 content but this is largely due to $NaR^{+++}Si_2O_6$ solid solution in the clinopyroxene. Neglecting the sodic pyroxene component, the orthopyroxene and clinopyroxene have very similar degrees of $(Ca, Mg)Al_2SiO_6$ solid solution. The orthopyroxenes crystallizing above $1300^\circ C$ and lying on the boundary LF contain $6.0 \pm 0.2\%$ Al_2O_3 .

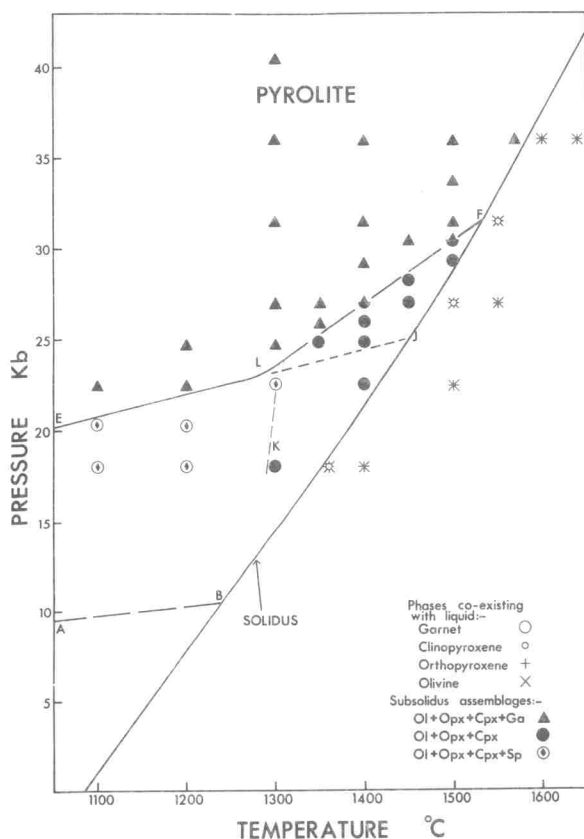


Fig. 1. Experimental runs on pyrolite III composition. Garnet is absent on the low pressure and present on the high pressure side of ELF. Spinel is absent on the high temperature side of the line K. In pyrolites I and II garnet is present on the high pressure side of ELJ.

Table 2

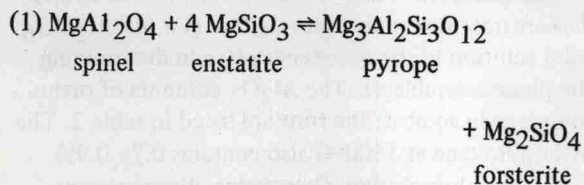
Alumina content of orthopyroxene in equilibrium with garnet in high pressure experimental runs.

Pressure	Temperature (°C)	Al ₂ O ₃ * content of orthopyroxene (weight percent)	Garnet content of assemblage	Spinel content
<i>Pyrolite III</i>				
24.8	1350	6.1	nil	nil
25.9	1350	5.5	minor	nil
27.0	1350	4.9	minor	nil
36.0	1300	2.6	common	nil
40.5	1300	2.2	common	nil
30.4	1500	5.9	trace	nil
31.5	1500	5.6	minor	nil
33.8	1500	4.8	minor	nil
36.0	1500	4.2	common	nil
<i>Pyrolite I</i>				
24.8	1400	5.9	trace	minor

* Estimated accuracy, ±5% of amount present.

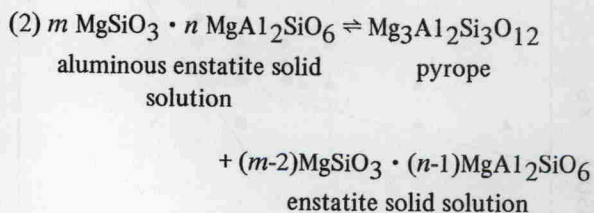
Preliminary curves denoting the maximum Al₂O₃ content of orthopyroxene in equilibrium with garnet in pyrolite compositions may be derived from the data of table 2 and have been shown in fig. 2.

The cause of the break in slope of the boundary ELF lies in the different equilibria involved in the formation of garnet along the curve. At temperatures below L, aluminous spinel is present in the assemblage and is in equilibrium with orthopyroxene containing Al₂O₃ < 6.0%. The first appearance of garnet from this assemblage involves reaction between spinel and pyroxenes [10] and the idealized reaction is as follows:



In contrast, spinel is absent above 1300°C in pyrolite III composition and the Al₂O₃ content of the mix is entirely in solid solution in the pyroxenes. In this assemblage the orthopyroxene contains 6% Al₂O₃ (weight percent) and the clinopyroxene contains > 6% Al₂O₃. Garnet appears from this assemblage when the load pressure is sufficient to cause the aluminous pyroxenes to break down in favour of

garnet + less-aluminous pyroxene [11, 12]. Thus the simplified reaction for the appearance of garnet in pyrolite III composition along LF is as follows:



The different roles of reactions involving spinel and those involving aluminous pyroxenes are in harmony with previous work on simple systems [10-14]. The boundary EJ (fig. 1) is almost identical to that established by MacGregor [10] for reaction (1) in the pure spinel + 4 enstatite system, provided that a -10% pressure correction is applied to MacGregor's data. The boundary LF representing assemblages containing garnet in equilibrium with orthopyroxene (6.0% Al₂O₃) is similar in slope to analogous boundaries in the pure magnesian system, enstatite + pyrope [12] and the natural, simple system enstatite + chromiferous pyrope garnet [11]. However, at a given pressure and temperature, the Al₂O₃-content of orthopyroxene in equilibrium with garnet in the complex pyrolite composition is substantially less than that obtained in the